JOURNAL OF MATERIALS SCIENCE 16 (1981) 1183–1186

Electrical conduction in evaporated terbium fluoride thin films

K. R. PARAMASIVAM, M. RADHAKRISHNAN, C. BALASUBRAMANIAN
Department of Physics, Madras University Autonomous Post-Graduate Centre, Coimbatore 641 041, India

The current–voltage characteristics of thin-film capacitors with evaporated terbium fluoride dielectric have been studied as a function of temperature (in the range 300 to 418 K). For sufficiently high electric fields ($> 10^4$ V cm^{-1}), the leakage current is found to increase exponentially with the square root of the applied electric field. Analysis of the data suggests an electrode-limited mechanism such as that suggested by Schottky. It is seen that the conduction mechanism is an activated process with the activation energy decreasing with increasing field. Dielectric break-down and its dependence on film thickness have also been investigated. Break-down field strength follows the Forlani–Minnaja relation.

1. Introduction

In recent years, considerable interest has been stimulated in the study of direct current conduction [1–3] and break-down phenomena [4, 5] in thin dielectric layers because of their use in passivated devices, field effect transistors and microcircuitry. Electrical conduction in rare-earth oxide films has been studied by various workers [6–8]. Terbium fluoride films have been previously studied to investigate the electroluminescence [9] and dielectric [10] properties. In the work reported here, an investigation of the current transport mechanisms in TbF_3 films as a function of applied voltage and temperature was performed. The dielectric strength, which is of considerable importance for device applications, has also been studied.

2. Experimental details

2.1. Fabrication of thin-film capacitors

Films were prepared by making use of a conventional 12-inch vacuum coating unit at a pressure of 2.5×10^{-5} Torr. Pure aluminium (99.999% purity) was evaporated from a tungsten filament onto precleaned glass substrates through suitable masks to form the base electrode. Terbium fluoride powder of 99.9% purity (obtained from Indian Rare-Earths Ltd.) was evaporated from a resistively heated molybdenum boat to form the dielectric layer. An aluminium counter electrode was evaporated onto the dielectric to form the MIM sandwich structure (Al–TbF_3–Al). The dielectric thickness was measured by a multiple-beam interferometer (Fizeau fringes). All the capacitors were stabilized by prolonged aging and repeated annealing cycles at about 100° C. The structure of the films has been identified as amorphous from X-ray diffraction studies [10].

2.2. Direct current conduction measurements

The current across the capacitor was measured in vacuo as a function of the applied voltage at different temperatures using a ECIL electrometer amplifier (Model EA815) and a FET nanoammeter (Aplab Model 5006). The temperature of the sample was determined using a previously-calibrated copper–constantan thermocouple.

2.3. Direct current break-down measurements

The capacitor was placed in series in a circuit consisting of a d.c. power supply, a potential divider, a standard resistor and a nanoammeter. As the voltage was increased in steps, the change in current was noted using the nanoammeter. The on-set break-down voltage, V_B, was detected by a sudden

0022–2461/81/051183–04$02.40/0

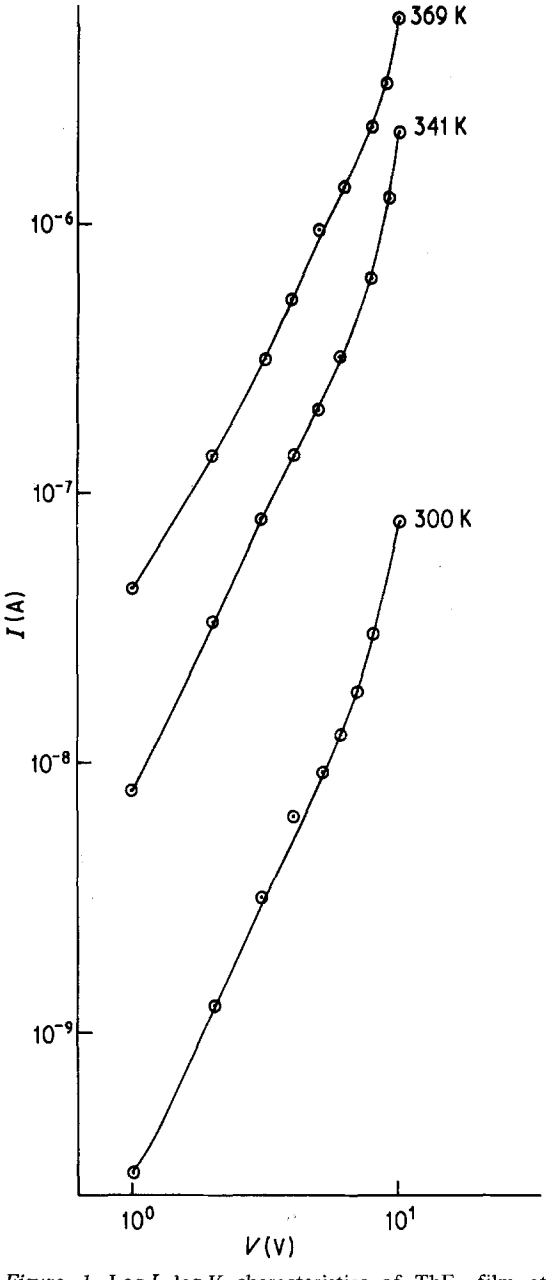

Figure 1 Log I–log V characteristics of TbF_3 film at different temperatures ($d = 155$ nm).

rise in the current observed in the nanoammeter. Measurements of the break-down voltage were carried out under vacuum with the samples of thicknesses in the range 30 to 260 nanometers.

3. Results and discussion

3.1. Direct current conduction

Log I–log V characteristics of terbium fluoride film of thickness 155 nm are presented in Fig. 1. The current, I, exhibits a voltage, V, dependence of the form $I \propto V^n$ where n is found to vary from

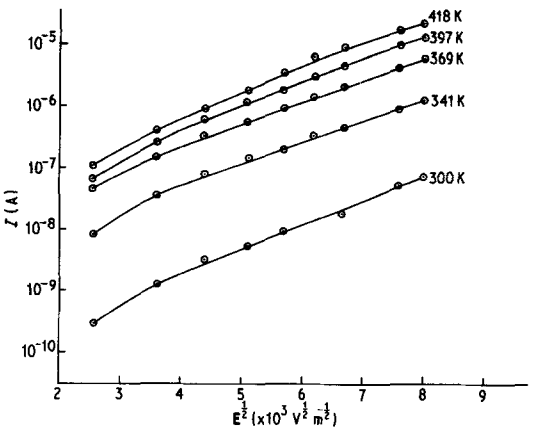

Figure 2 Log I plotted against $E^{1/2}$ for a TbF_3 film at various temperatures ($d = 155$ nm).

1.8 at moderate fields to greater than 5 at high fields. When referring to power-law dependence of current upon voltage in the context of dielectric films, one naturally tends to think of space-charge-limited flow in solids [11]. For space-charge-limited conductivity, the current, I, is related to the applied voltage, V, by

$$I = K\frac{V^2}{d^3} \qquad (1)$$

where K is a constant and d is the thickness of the dielectric film. For the case of TbF_3 films, it is verified that the above equation is not followed; Also, the observed current variations (Fig. 1.) are more rapid than those predicted by the square-power law. Hence, the possibility of space-charge-limited conduction is ruled out for TbF_3 films.

Fig. 2. represents the variation of current with the square root of the field. The curves show slight deviation from straight-line characteristics at low fields and this has been attributed to contact potential effects [12]. The straight-line nature of the curves at high fields may be explained by a Poole–Frenkel bulk mechanism or by Schottky emission at the electrodes. In the Poole–Frenkel process, the conduction is limited by the field-enhanced thermal emission of electrons from a discrete trap level into the conduction band. In the Schottky emission mechanism, electrons are emitted from the metal electrode into the conduction band of the insulating film over the image force interfacial barrier under attendant lowering of the applied electric field. It is a well-established experimental fact that at fields greater than 10^4 V cm^{-1} many dielectric films exhibit a current–voltage relationship characteristic of the form [11, 13]

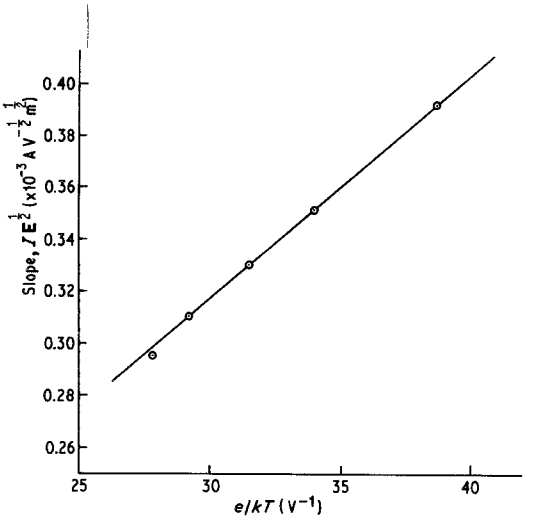

Figure 3 The slope of the curves, $IE^{1/2}$, shown in Fig. 2 plotted against e/kT.

$$I = I_0 \exp\left[\frac{e\beta E^{1/2}}{kT}\right], \qquad (2)$$

where $E = V/d$ and β is a constant given by

$$\beta = \left[\frac{e}{a\pi\epsilon_0\epsilon'}\right]^{1/2}, \qquad (3)$$

e is the electronic charge, ϵ_0 is the permittivity of free space and ϵ' is the high-frequency dielectric constant. The value of $a = 1$ is adopted for Poole–Frenkel emission and the value of $a = 4$ is adopted for Schottky emission. Since ϵ' appears to the power one half in Equation 3, it can be considered to be of secondary importance as far as its effect on the theoretical magnitude of β is concerned [14]. In the present investigation, the high-frequency dielectric constant of 5.1, calculated from the usual parallel-plate formula, has been used for the evaluation of β, using Equation 3.

The slopes of the straight lines in Fig. 2 are plotted against e/kT in Fig. 3. The slope of the curve in Fig. 3 yields the experimental value of β [11]. The calculated and observed values of β are

$$\beta_S = 1.68 \times 10^{-5}\ (\mathrm{mV})^{1/2};$$

$$\beta_{PF} = 3.36 \times 10^{-5}\ (\mathrm{mV})^{1/2};$$

$$\beta_{expt} = 1.96 \times 10^{-5}\ (\mathrm{mV})^{1/2}.$$

Since the value of β_{expt} is closer to that of β_S than β_{PF}, the conduction mechanism seems to be predominantly that of Schottky emission for the temperature range studied (300–418 K). Also, the Schottky plots of $\log I/T^2$ against $1/T$ at different voltages (Fig. 4) yield straight lines confirming the Schottky type of conduction mechanism [15].

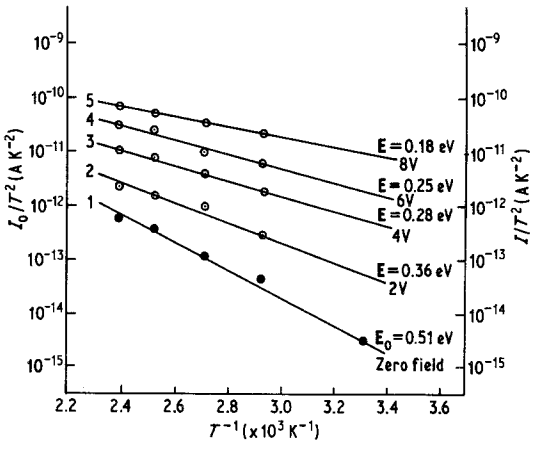

Figure 4 (a) Plot of $\log I_0/T^2$ against T^{-1} (closed circles) (b) Plot of $\log I/T^2$ against $1/T$ at various voltages (open circles).

Curve 1 in Fig. 4 represents the variation of $\log I_0/T^2$ (I_0 is the current intercept corresponding to $V = 0$ in Fig. 2) with inverse absolute temperature. The zero-field activation energy, evaluated from the slope of this curve, is 0.51 eV. Curves 2 to 5 in Fig. 4 are plots of $\log I/T^2$ against $1/T$ at different voltages. The resulting activation energies are plotted against $V^{1/2}$ (Fig. 5) and, by extrapolation, the zero-field activation energy has been found to be 0.52 eV. From Fig. 4, it is evident that the conduction mechanism is an activated process

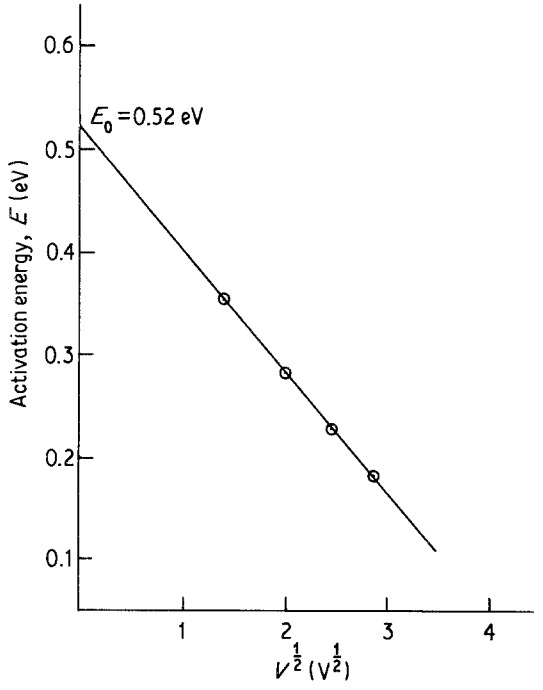

Figure 5 Activation energy, E, plotted against square root of applied voltage, $V^{1/2}$.

TABLE I Variation of breakdown voltage, V_B, and dielectric field strength, E_B, with film thickness

Thickness, d (nm)	Breakdown voltage, V_B (V)	Dielectric field strength, E_B ($\times 10^6$ V cm^{-1})
30.0	13	4.33
50.0	18	3.60
90.0	24	2.66
105.0	26	2.48
155.0	33	2.13
184.4	36	1.95
260.0	43	1.65

with the activation energy decreasing with increasing field. Similar results have been obtained by several workers [16–18] for different insulating films.

3.2. Break-down voltage and field strength

It is observed that the onset break-down voltage, V_B, increases from 13 V to 43 V with the increase of film thickness, d, from 30 to 260 nm, whereas the field strength E_B ($E_B = V_B/d$) decreases from 4.33×10^6 to 1.65×10^6 V cm^{-1} (see Table I). Fig. 6 shows a plot of log E_B against log d and the slope of the curve is found to be -0.47, thus obeying the Forlani–Minnaja law, $E_B \propto d^{-1/2}$ [12, 20]. Similar thickness dependence behaviour in other insulating films has been reported by several workers [21–23].

4. Conclusions

The current–voltage characteristics for evaporated TbF_3 films sandwiched between aluminium electrodes are suggestive of Schottky emission. The results show a definite lowering of the activation energy for the conduction process with the field. The break-down field is found to be a power-dependent function of dielectric thickness, as predicted by Forlani and Minnaja.

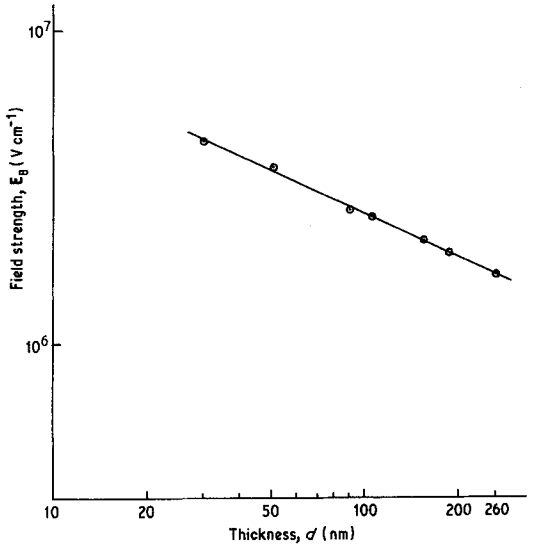

Figure 6 Variation of E_B with thickness, d.

Acknowledgements

One of the authors (KRP) is thankful to Chikkaiah Naicker College, Erode and the University Grants Commission, New Delhi for the deputation under the Faculty Improvement Programme.

References

1. D. L. PULFREY, A. H. M. SHOUSHA and L. YOUNG, *J. Appl. Phys.* **41** (1970) 2838.
2. L. SULLIVAN and H. C. CARD, *J. Phys. D* **7** (1974) 1531.
3. A. M. PHAHLE, *Thin Solid Films* **46** (1977) 315.
4. N. KLEIN, *ibid.* **7** (1971) 149.
5. V. K. AGARWAL and V. K. SRIVASTAVA, *ibid.* **8** (1971) 377.
6. A. T. FROMHOLD, Jr, *Phys. Stat. Solidi* **36** (1969) K129.
7. M. SAYER, M. SUZANNE MARTIN and N. J. HELLICAR, *Thin Solid Films* **6** (1970) R61.
8. E. RIEMANN and L. YOUNG, *J. Appl. Phys.* **44** (1973) 1044.
9. T. YABUMOTO, H. MATSUMOTO and S. MARUI, *Japan. J. Appl. Phys.* **11** (1972) 1858.
10. K. R. PARAMASIVAM, M. RADHAKRISHNAN and C. BALASUBRAMANIAN, *Thin Solid Films* **14** (1980) 189.
11. A. K. JONSCHER, *ibid.* **1** (1967) 213.
12. A. E. HILL, A. M. PHAHLE and J. H. CALDERWOOD, *ibid.* **5** (1970) 287.
13. A. SERVINI and A. K. JONSCHER, *ibid.* **3** (1969) 341.
14. V. K. AGARWAL and H. MITSUHASHI, *ibid.* **41** (1977) 271.
15. P. J. REUCROFT and S. K. GHOSH, *ibid.* **20** (1974) 363.
16. D. M. HUGHES and M. W. JONES, *J. Phys. D* **7** (1974) 2081.
17. M. J. RAND and J. F. ROBERTS, *J. Electrochem. Soc.* **115** (1968) 423.
18. H. HIROSE and Y. WADA, *Japan J. Apply. Phys.* **4** (1965) 639.
19. F. FORLANI and N. MINNAJA, *Phys. Stat. Solidi* **4** (1964) 311.
20. *Idem, J. Vac. Sci. Technol.* **6** (1969) 518.
21. P. P. BUDENSTEIN, P. J. HAYES, J. L. SMITH and W. B. SMITH, *ibid.* **6** (1969) 289.
22. A. GOSWAMI and A. P. GOSWAMI, *Thin Solid Films* **16** (1973) 175.
23. V. K. AGARWAL and V. K. SRIVASTAVA, *ibid.* **13** (1972) S23.

Received 11 August and accepted 15 September 1980.